Proceedings of the International Conference on Heat Exchanger Fouling and Cleaning - 2024 (Peer-reviewed)
April 21–26, 2024, Lisbon, Portugal; Editors: H.U. Zettler and E.M. Ishiyama

A COMPARATIVE EVALUATION OF INHIBITOR PERFORMANCE IN SIMPLE AND COMPLEX SOLUTIONS

***I.A. Løge[1], and B.U. Anabaraonye[2]**

[1] Department of Chemical and Biochemical Engineering, Technical University of Denmark, Søltofts Plads 2800 Kongens Lyngby, Denmark, isacl@kt.dtu.dk

[2] Danish Offshore Technology Centre, Technical University of Denmark, Elektrovej, 2800 Kongens Lyngby, Denmark

ABSTRACT

Crystallization fouling is a major challenge in heat exchangers as it causes a decreased in efficiency. Mitigating this challenge is therefore critical and chemical inhibitors are widely used for this purpose. However, the use of chemical inhibitors could pose environmental concerns. To optimally utilize inhibitors, it is essential to understand their underlying mechanisms. In this study, we investigated the performance of a commercial chemical inhibitor in single and complex (multi-component) brines. Surface deposition studies were performed in a tubular reactor and the deposits were analyzed using X-ray CT scanning and metrology parameters. We observe that inhibitor concentration and brine composition have a significant effect on the deposition rates and crystal habit.

INTRODUCTION

Fouling remains an unresolved challenge in the operation of heat exchangers[1]. The detrimental effects of fouling are well documented, including reduced heat transfer efficiency, higher operating pressure, and blockage of flow lines, these lead to increased energy consumption and operational costs [2]. For these reasons, mitigation strategies are important. Despite advances in understanding fouling mechanisms [3,4] and the development of mitigation strategies, such as the use of inhibitors [5], the effectiveness of these strategies is system-dependent.

Inhibitors can alter sub-processes in the fouling processes including nucleation, crystal growth, and adhesion. An important to question to address is: do inhibitors exhibit similar behavior in simple and complex (multi-component) brine solutions?

Despite the critical importance of this question, there is a significant gap in the literature regarding the comparative evaluation of inhibitor performance in simple and complex solutions. Although numerous studies have explored inhibitor efficiency in controlled environments[6], few have ventured into the realm of complex process streams representative of industrial applications[7,8]. Addressing this gap is essential for improving our understanding of fouling mitigation strategies and facilitating their practical implementation.

MATERIALS AND METHOD

We used a commercial carboxylic acid polymer inhibitor at inhibitor concentrations of 0, 1, and 10 ppm. Simple brines and complex brines were prepared. The compositions of the brines can be found in Tables 1 and 2, respectively.

Table 1. Chemical compositions of simple brines (SB)

SB 1 (g/kg H_2O)		SB 2 (g/kg H_2O)	
Na_2SO_4	[0.07,0.12]	$BaCl_2.2H_2O$	[0.12, 0.21]

Table 1. Chemical compositions of complex brines (CB)

CB 1 (g/kg H_2O)		CB 2 (g/kg H_2O)	
NaCl	59.63	KCl	1.17
Na_2SO_4	4.51	$MgCl_2.6H_2O$	13.14
		$CaCl_2.2H_2O$	2.56
		$SrCl_2.6H_2O$	0.22
		$BaCl_2.2H_2O$	[0.12, 0.25]

The saturation ratios (SR), for each solution after mixing the brines in a 1:1 ratio, were calculated using the PHREEQC geochemical simulator and implementing Pitzer parameters. *SR* is defined as:

$$SR = \frac{a_i * a_j}{K_{SP}}$$

where a_i and a_j are the activities of the reactants and K_{SP} is the solubility constant. The calculated SR values for all experiments are shown in Table 3.

Experimental Procedure

The setup for the surface deposition experiments is identical to the one used in our previous studies[9]. The deposition cells are lathed on a CNC machine in an in-house workshop and made of Uddeholm Bure steel. The areas in contact with the brine solution had an inner diameter of 3 mm and

ISBN: 978-0-9984188-3-4; Published online www.heatexchanger-fouling.com

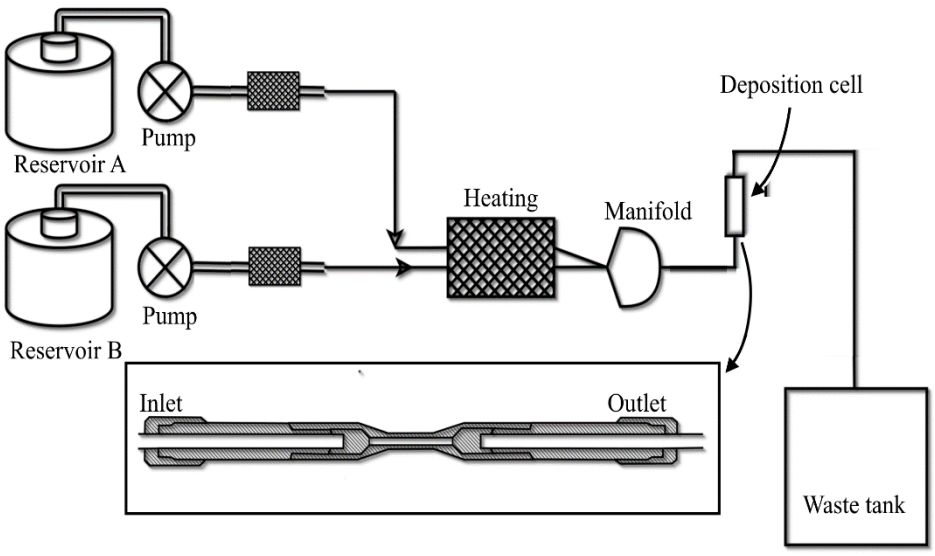

Figure 1: Schematic of experimental set-up.

a length of 3 cm. The solution temperature was fixed at 80 ° C, and the solution was heated with a heating bath. The deposition cell was thermally isolated. The flow rate for each brine was 80 ml / min, which ensures a Reynolds number of 4808 within the deposition cell. Each flow experiment was designed to inject a total of 7.2 mmol of Ba^{2+} by the end. Brines were injected at a 1:1 volumetric ratio. The rate is determined from the weight difference of the deposition cell before and after injection. A new deposition cell is used for each experiment. The deposition cells were then imaged in the CT scanner after each experiment. The presented methodology has been previously shown to result in accurate data, with a relative standard deviation of 2.9%[10].

Characterization of surface features

X-ray Imaging

We used a ZEISS Xradia 410 Versa for X-ray CT scanning. This system, equipped with an HE1 (high energy) filter, operates at a voltage of 150 kV. Tomograms were generated from 1608 projections, each with a 1-second exposure time and a voxel resolution of 8.0 μm. These projections were processed into reconstructed images using the system's integrated software.

Processing of images

Segmentation was performed in Avizo 2021 through thresholding. The scale and steel were differentiated from ambient air. This segmentation process involved rescaling the images to a resolution of 19.2 μm and compiling them into a stack of image files. To remove artefacts from reconstruction, the first and last 25 images of each stack were removed.

Texture parameters

Following the approach developed by Klingaa et al.[12] and used in our previous studies [13]. Surface textures were analyzed to determine texture parameters. Using the compiled image stacks, both surface and profile textures were evaluated. In this work, we present surface spikiness (Sku)

$$\mathrm{Sku} = \frac{1}{\mathrm{Sq}^4}\left(\frac{1}{\mathrm{l}}\int_0^{\mathrm{l}} \mathrm{Z(x,y)}^4 \mathrm{dxdy}\right)$$

Where Sq is the root mean square of the heigh distribution (Z(x,y)) and l is the width and breadth of surface.

Furthermore, we use the average of the ten most significant valley-to-peak measurements (P10z):

$$\mathrm{P10z} = \frac{1}{10}\left(\sum_{\mathrm{i=1}}^{10} \max_{10}[\mathrm{Z(x)}]_{\mathrm{i}} - \min_{10}[\mathrm{Z(x)}]_{\mathrm{i}}\right)$$

P10z is used to describe the height of the crystals and presented in subsequent figures as Height.

These can provide insight into the size and nature of surface irregularities. Previous studies have highlighted the value of these texture parameters in assessing the development of fouling[14].

Surface Coverage

A MATLAB script was used to analyze surface coverage, using CT reconstructed images as inputs. By slicing each tomogram vertically, the inner circumference of each slice was mapped, dividing it into 2000 segments. A calculation of pixel intensity sums was performed from the center of the outer edge at a depth of 0.3 radius. Based on the sum of the pixel intensity, a threshold was applied to determine whether a surface was scaled or not.

ISBN: 978-0-9984188-3-4; Published online www.heatexchanger-fouling.com

Table 3 Calculated saturation ratios for this study

System	Na_2SO_4 (g/kg H_2O)	$BaCl_2$ (g/kg H_2O)	SR
Simple brine	0.07	0.12	134.9
Simple brine	0.12	0.21	380.2
Complex brine	4.51	0.12	135.0
Complex brine	4.51	0.25	302.0

RESULTS & DISCUSSION

Gravimetric analysis

Crystal growth in simple and complex brines has different behaviors under varying conditions (Figure 2). In simple brines, crystal deposition was minimal at the lowest SR studied (SR=138), with a slight decrease in deposited mass as inhibitor concentration increased (Figure 2**a**). At a higher SR (380, Figure 2**b**), we observe an overall increase in deposition rates, compared to the lower SR systems. We also observe a continuous decrease in deposition rates as inhibitor concentrations are increased.

In the complex brine system, at SR=135, the deposition rates also decreased as inhibitor concentrations increased. However, at an SR of 302, the deposition rate increased in the presence of an

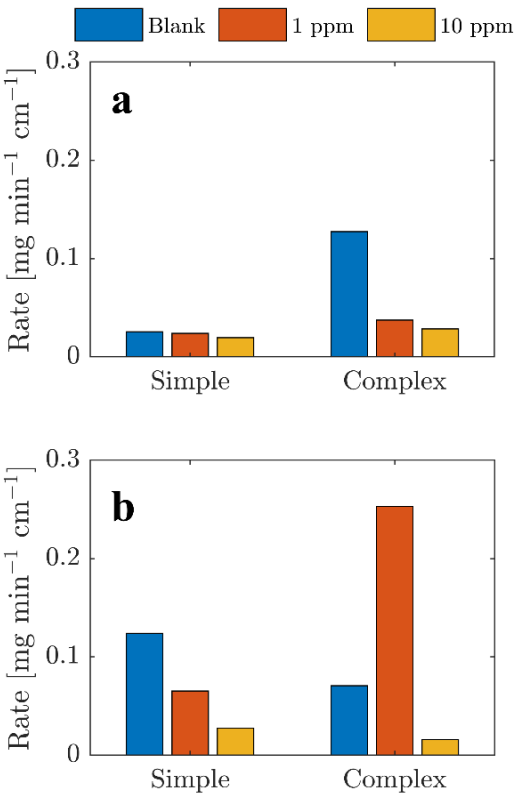

Figure 2: Deposition rates of $BaSO_4$ crystals precipitated from low (a) and high (b) SR. See specific SR values in Table 3.

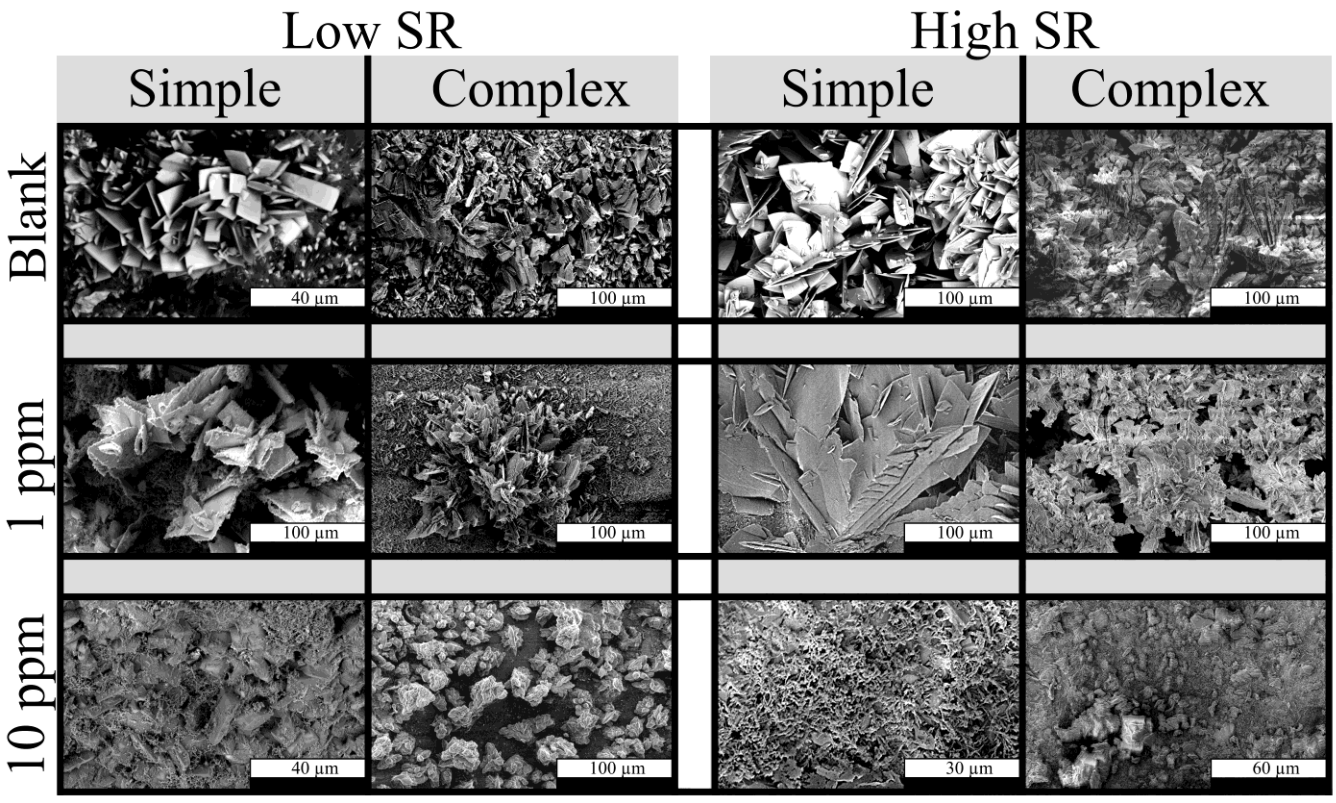

Figure 3: Scanning electron microscopy of adhered strucures deposited from simple and complex solutions, with 0 (blank), 1, and, 10 ppm inhibitor.

ISBN: 978-0-9984188-3-4; Published online www.heatexchanger-fouling.com

inhibitor concentration of 1 ppm. This aligns with our previous studies[11]. We demonstrated that inhibitors at certain concentrations, could alter crystals properties in such a way that detachment processes are delayed, thereby leading to an overall increase in deposition rate.

Crystals formed from the complex brines tend to be more compact and resemble dandelion leaves rather than simple plates. While these crystals appear denser, similar to those formed in the simple brines, they become larger as saturation ratios increased. Crystals formed from complex solutions

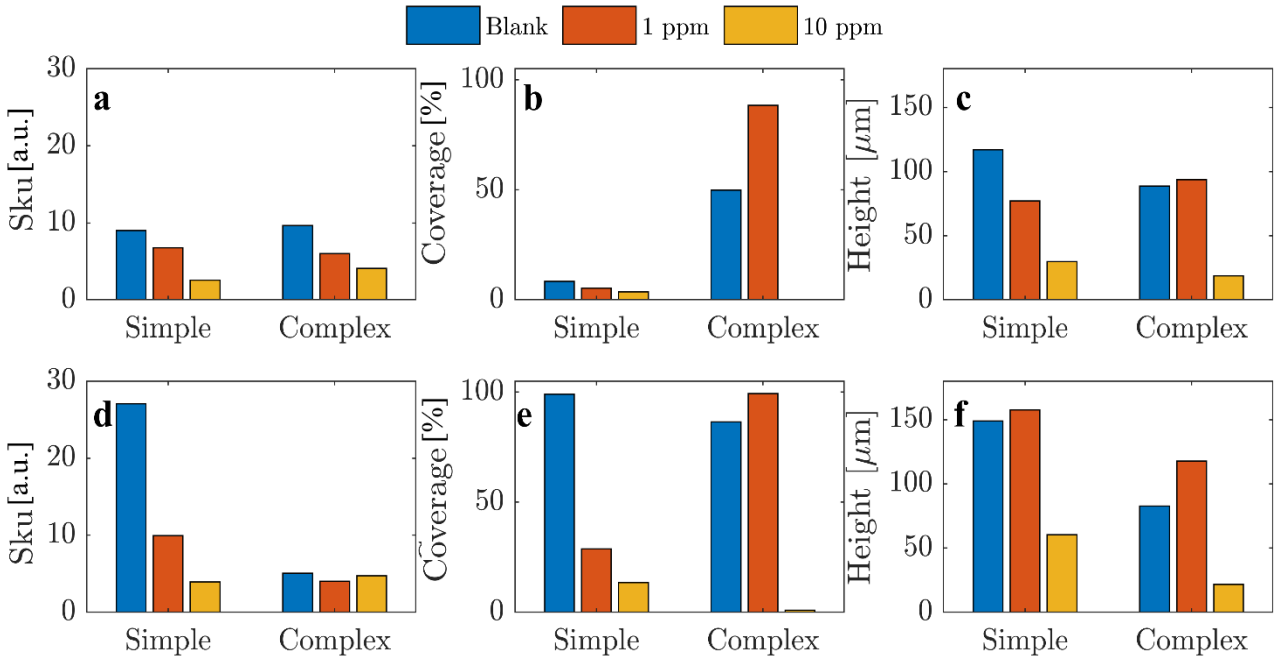

Figure 4: Texture parameters of crystals formed from **a-c** low and **d-f** high SR solutions.

Microstructure analysis

Both inhibitor concentration and brine composition can significantly influence the shape of crystal structures. The shape of the crystal structures dictates the adherence of deposits to a surface, for instance, tall individual structures are more susceptible to detachment processes. Therefore, investigating deposits on a microscopic scale using scanning electron microscopy is useful for better understanding the mechanism of the inhibitor.

Figure 3 shows the crystal habits in the present study. In simple brine systems, without an inhibitor present, $BaSO_4$ crystals display plate-like structures. We observe that crystals formed at higher concentrations are much larger (see scalebars in Figure 3).

In the presence of the inhibitor, the crystals gradually become smaller and have fewer well-defined faces. At an inhibitor concentration of 10 ppm, the deposited crystals are much smaller and have completely changed their crystal habit. These results are consistent with previous studies that have shown that crystals lose their well-defined morphology in the presence of a chemical inhibitor [15].

also lose their dimensionality in the presence of a chemical inhibitor. Notably, these crystals maintain a higher degree of dimensionality in the presence of the inhibitor, compared to crystals formed from a simple solution. This is evident at 10 ppm and SR ≈ 300, the crystals formed from the simple solution display thread-like structures, while rhomboidal structures remain for crystals formed from the complex solution.

Surface analysis through texture parameters

Texture parameters are useful for understanding the mechanism of deposition. They provide insight into the shape of crystals on a surface, which determines their resilience toward detachment. For example, crystals that are distributed far from each other, with high spikiness (Sku), are more likely to detach from the surface, resulting in lower net deposition over time[10].

In most cases, deposits show lower spikiness (Sku) when more inhibitor is added (Figure 4a, 4d). A spiky deposition is evidence of nucleation-driven deposition; therefore, a lowered spikiness indicates that the inhibitor decreases the driving force for nucleation processes[4]. This is also visible for the deposition formed under simple brine conditions, namely, that at higher saturation ratios, there is a higher spikiness. However, this is not the case for

ISBN: 978-0-9984188-3-4; Published online www.heatexchanger-fouling.com

deposition formed from complex brines. The growth is less spiky at an SR of 302 compared to that of 135.

Although deposits formed in complex brine systems had a lower spikiness than those of simple brine, they cover a significantly larger area. For instance, deposition at an SR of 135 from the simple brine system had surface coverage values close to 10 %, while at SR values, deposits from the complex brine system had surface coverages of 50% and 90% (Figure 4b). It appears that the presence of other ions have significantly changed the way the surface is covered. Our method did not capture the surface coverage of the deposits at the highest inhibitor concentrations for the complex brine systems.

The heights of the crystals were estimated through the texture parameter, P10z. P10z is the mean value of the 10 largest valley-to-peak values and therefore represents the tallest crystals formed. In simple brines systems, the deposits grew taller at higher saturation ratios, and overall, the presence of the inhibitor decreased the heights of the deposits. In the complex brine systems, at 1 ppm inhibitor concentration, an increase in height is observed at both saturation ratios, at 10 ppm inhibitor concentration, there is a marked decrease in the heights of the deposits.

The comparison of the gravimetric data (Figure 2) and the texture analysis (Figure 4), shows how the mass is distributed. While deposition rates are similar in magnitude for the simple and complex brines at low supersaturation, their coverages are not. As the coverage of the crystals formed from the complex solution has a higher coverage, it suggests evidence that the crystals formed are more spread out on the surface. The crystal heights (Figure 4**c**) are also slightly lower for crystals formed from the complex. The high coverage, and lower heights, indicate that crystals have formed adhered to the surface.

CONCLUSION

We use gravimetric analysis, microscopy, and texture parameters based on X-ray CT scans to demonstrate that the effect of chemical inhibitors $BaSO_4$ deposition depends on the chemistry of the brine system.

Generally, there is a decrease in spikiness with inhibitor concentration except for deposits formed in the complex brine systems at high SR values. Spikiness increases in simple systems with higher SR, while the reverse is observed for deposits formed from simple brine systems. In most cases, deposits formed from the simple brine systems cover smaller areas of the surface, than their counterparts formed from complex brine systems. This contrasts with the mass deposited, where the deposition of the complex solution at the low SR was the largest. A comparative analysis of the mass and texture parameters allows us to observed that crystal forming from complex solutions are more compact and have close adherence to the surface.

REFERENCES

1. Berce, J., Zupančič, M., Može, M. & Golobič, I. A review of crystallization fouling in heat exchangers. *Processes* **9**, (2021).
2. Müller-Steinhagen, H. Cooling-Water Fouling in Heat Exchangers. *Adv. Heat Transf.* (1999) doi:10.1016/S0065-2717(08)70307-1.
3. Løge, I. A. *et al.* Revealing the complex spatiotemporal nature of crystal growth in a steel pipe: Initiation, expansion, and densification. *Chem. Eng. J.* **466**, 143157 (2023).
4. Løge, I. A., Anabaraonye, B. U., Bovet, N. & Fosbøl, P. L. Crystal Nucleation and Growth: Supersaturation and Crystal Resilience Determine Stickability. *Cryst. Growth Des.* **23**, 2619–2627 (2023).
5. Xiao, J., Kan, A. T. & Tomson, M. B. Prediction of BaSo4 precipitation in the presence and absence of a polymeric inhibitor: Phosphino-polycarboxylic acid. *Langmuir* **17**, 4668–4673 (2001).
6. Sorbie, K. S. & Laing, N. How scale inhibitors work: Mechanisms of selected barium sulphate scale inhibitors across a wide temperature range. *Proc. - SPE Sixth Int. Symp. Oilf. Scale; Explor. Boundaries Scale Control* 447–456 (2004) doi:10.2118/87470-ms.
7. Wang, Z., Neville, A. & Meredith, A. W. How and why does scale stick - Can the surface be engineered to decrease scale formation and adhesion? *SPE Seventh Int. Symp. Oilf. Scale 2005 Push. Boundaries Scale Control. Proc.* 85–92 (2005) doi:10.2118/94993-ms.
8. Boak, L. S., Graham, G. M. & Sorbie, K. S. Influence of divalent cations on the performance of BaSO 4 scale inhibitor species. *Proc. - SPE Int. Symp. Oilf. Chem.* 643–648 (1999) doi:10.2118/50771-ms.
9. Løge, I. A., Anabaraonye, B. U., Bovet, N. & Fosbøl, P. L. Crystal Nucleation and Growth: Supersaturation and Crystal Resilience Determine Stickability. *Cryst. Growth Des.* (2023) doi:10.1021/acs.cgd.2c01459.
10. Løge, I. A. *et al.* Scale attachment and detachment: The role of hydrodynamics and surface morphology. *Chem. Eng. J.*

ISBN: 978-0-9984188-3-4; Published online www.heatexchanger-fouling.com

430, 132583 (2021).
11. Løge, I. A., Dragani, T. & Anabaraonye, B. U. Decoupling Inhibitor Mechanisms in Surface and Bulk Processes: Studies of BaSO 4. *Cryst. Growth Des.* **23**, 8518–8526 (2023).
12. Klingaa, C. G., Dahmen, T., Baier, S., Mohanty, S. & Hattel, J. H. X-ray CT and image analysis methodology for local roughness characterization in cooling channels made by metal additive manufacturing. *Addit. Manuf.* **32**, 101032 (2020).
13. Appelquist Løge, I., Winkel Rasmussen, P., Neerup, R. & Fosbøl, P. L. In-Situ Measurements of Mineral Precipitation by Means of CT-Scanning. *SSRN Electron. J.* (2022) doi:10.2139/ssrn.4276122.
14. Løge, I. A., Neerup, R. & Fosbøl, P. L. A New View on Scale. *Soc. Pet. Eng. - SPE Int. Oilf. Scale Conf. Exhib. OSS 2022* 25–26 (2022) doi:10.2118/209512-MS.
15. Benton, W. J., Collins, I. R., Grimsey, I. M., Parkinson, G. M. & Rodger, S. A. Nucleation, growth and inhibition of barium sulfate-controlled modification with organic and inorganic additives. *Faraday Discuss.* **95**, 281–297 (1993).

ISBN: 978-0-9984188-3-4; Published online www.heatexchanger-fouling.com